Separation Science and Technology
Publication details, including instructions for authors and subscription information:
http://www.informaworld.com/smpp/title~content=t713708471

Molecular Imprinting by 4-Hydroxybenzoic Acid: A Two-Site Model

Lucy Yue Hu[a]; Robert A. Orwoll[a]
[a] Departments of Applied Science and Chemistry, College of William and Mary, Williamsburg, VA, USA

Online publication date: 29 November 2010

To cite this Article Hu, Lucy Yue and Orwoll, Robert A.(2010) 'Molecular Imprinting by 4-Hydroxybenzoic Acid: A Two-Site Model', Separation Science and Technology, 45: 16, 2337 — 2344
To link to this Article: DOI: 10.1080/01496395.2010.491811
URL: http://dx.doi.org/10.1080/01496395.2010.491811

Separation Science and Technology, 45: 2337–2344, 2010

ISSN: 0149-6395 print/1520-5754 online
DOI: 10.1080/01496395.2010.491811

Taylor & Francis
Taylor & Francis Group

Molecular Imprinting by 4-Hydroxybenzoic Acid: A Two-Site Model

Lucy Yue Hu and Robert A. Orwoll
Departments of Applied Science and Chemistry, College of William and Mary, Williamsburg, VA, USA

4-Hydroxybenzoic acid (4HBA) imprinted polymer was synthesized with the functional monomer, acrylamide, and the crosslinking agent, ethylene glycol dimethacrylate, in acetonitrile. Hydrogen bonding between the template and the monomer not only controls the template molecules in and out of the binding sites, but also contributes to special binding sites in the resulting polymer resin. Batch analyses showed that the 4HBA-imprinted polymer has a special affinity for the *para*-substituted hydroxybenzoic acid, but not for its *meta*-substituted isomer (3HBA), nor for benzoic acid (BA). The binding behavior of 4HBA can be interpreted with a simple two-site model with one kind of site in the resin being special for 4HBA and the other kind being general with similar affinities for 4HBA, 3HBA, and BA. These general binding sites found in both the imprinted resin and the non-imprinted reference resin have greater affinity, but are less numerous than the sites unique to the imprinted resin.

Keywords 4-hydroxybenzoic acid (4HBA); binding affinity; hydrogen bonding; molecular imprinting; two-site model

INTRODUCTION

Molecular imprinting has been widely accepted in various disciplines with most of the research mainly focused on the utility of the method, addressing its effectiveness as a tool for the separation and identification of drugs (1,2), herbicides (3,4), metal ions (5), micro-organisms (6), proteins (7,8), steroids (9), amino acids (10,11), sugars (12), nuclei acids and their derivatives (13), and polynuclear aromatic hydrocarbons (14). However, in the recognition-based applications of molecularly imprinted polymers (MIPs), a notable difficulty is the low yield of high affinity binding sites (15). Other difficulties reside in the understanding and characterization of the binding sites in MIPs.

In attempts to understand the phenomenon of molecular imprinting by modeling, the Scatchard method (16) is commonly employed, either the simple form in which only one kind of binding site is identified or a Scatchard-like treatment of two independent classes of binding sites. In the second case, the analyses have treated one kind of binding over one range of concentration and the second kind of binding over a different range of concentration, rather than both over the continuum of concentrations. In another attempt to model molecular imprinting, the affinity-spectrum approach (17–21) heavily emphasizes the distribution of binding affinities among the sites in an MIP resin and results in a complex mathematical model.

In general, MIPs are prepared by copolymerizing a suitable monomer and a crosslinking reagent in the presence of a nonreacting template species. The template is then extracted from the resulting resin, leaving behind sites that are especially suited for binding to that template species. The resin can then be used in chromatographic and batch analyses. A control resin, or non-imprinted polymer (NIP), is also prepared by the same procedure in the absence of a template and is typically used for comparing binding behaviors with MIP. Notwithstanding the important fact that the NIP also binds solute species, only rarely have investigators included the NIP in the binding affinity studies of imprinted systems quantitatively. Some studies (22–25) only reported binding isotherms for MIP and NIP without further analyses. Others either analyzed binding parameters, i.e., the association constant K_a and the density of the binding sites, of MIP and NIP independently (26), or artificially divided the concentration range into two distinct regions, followed by subtracting the NIP isotherm from the MIP isotherm to yield separate K_a values for binding in each concentration range (27,28).

The phenolic compounds have attracted interest for both the food and pharmaceutical industries due to their antioxidant properties. In the food production, such as wine and olive oil, these compounds are the main pollutants in its liquid waste (20). Among the wide group of phenolic compounds, 4-hydroxybenzoic acid is one of the simple forms. It has been imprinted using a monomer, either 4-vinylpyridine or acylamide, in the solvent mixture of either toluene/dodecanol (29) or methanol/water (30) in

Received 17 January 2010; accepted 5 May 2010.
Address correspondence to Lucy Yue Hu, Departments of Applied Science and Chemistry, College of William and Mary, Williamsburg, VA, USA. E-mail: lucyyuehu@gmail.com

an ultrasonic bath by thermal polymerization. Their binding behavior was examined via chromatography. In this paper, 4-hydroxybenzoic acid imprinted polymer and its reference NIP are polymerized in acetonitrile by ultraviolet initiation. Based on their equilibrium binding and selectivity properties, a simple two-site model is proposed which modifies the Scatchard-like treatment of two independent classes of binding sites so that both classes of binding sites are operative over the full range of concentrations.

EXPERIMENTAL

Materials and Reagents

4-Hydroxybenzoic acid (4HBA), 3-hydroxybenzoic acid (3HBA), benzoic acid (BA), ethylene glycol dimethacrylate (EGDMA), and 2,2′-azobisisobutyronitrile (AIBN) were purchased from Aldrich. Acrylamide (AA) was purchased from Bio-Rad Laboratories. Acetonitrile was of HPLC grade. All the other reagents were of analytical grade.

After being washed with a 15% aqueous sodium hydroxide solution and then saturated sodium bicarbonate solution, EGDMA was dried over calcium chloride and subsequently with calcium hydride. Before use, EGDMA was distilled *in vacuo* from calcium hydride and its purity was checked by gas chromatography/mass spectrometry. AIBN was recrystallized from methanol before use and acetonitrile was dried over 4 Å molecular sieves.

INTERACTION STUDY BETWEEN 4HBA AND AA BY TITRATION EXPERIMENT VIA ^{1}H-NMR

Stock solutions of 4HBA (0.1 mol/L) and AA (1.6 mol/L) were prepared in deuterated acetonitrile (CD_3CN). 0.40 mL of the 4HBA solution was pipetted into NMR tubes, and different volumes of AA and CD_3CN were added to yield ratios of AA (varying concentrations) to 4HBA (0.05 mol/L) ranging from 2 to 16 in a total volume of 0.80 mL. Also, for controls, the proton spectra obtained from a series of solutions containing only AA in CD_3CN were at the same concentrations as the AA concentrations in the 4HBA-AA solutions. All ^{1}H-NMR spectra were obtained at a normal probe temperature through a Gemini NMR 400, and the chemical shifts were reported in ppm (δ) with tetramethylsilane as an internal reference.

Preparation of MIP with 4HBA (MIP4HBA) and Non-Imprinted Polymer (NIP)

After 4HBA (the template; 0.1380 g, 1.0 mmol) had been dissolved in 5.00 mL acetonitrile, AA (the monomer; 0.4260 g, 6.0 mmol), EGDMA (the crosslinker; 5.70 mL, 30.0 mmol), and AIBN (the initiator; 0.0301 g, 0.18 mmol) were combined in a 50-mL flask. Then another 5.00 mL acetonitrile was added. The mixture was transferred into an 18 mm OD × 180 mm long borosilicate glass tube containing a small Teflon coated magnet. After it was sparged with nitrogen for 20 min, the sample was degassed three times by alternately submerging the tube in liquid nitrogen, reducing the pressure to 0.06 Torr for at least 15 min and then thawing. While thawing, a magnetic rod was used to move the small magnet up and down for the removal of bubbles from the solution. Following the above treatments, the tube was sealed at low pressure.

A second tube was prepared according to the same procedure but without the 4HBA template. The resulting resin is designated NIP. The amount of functional monomer used for synthesis of NIP was the same as that for the MIP to ensure that the differences in selectivity would not result from differences in functional groups concentrations.

The two sealed tubes were cooled to 4°C, agitated for 20 min, and then irradiated together for 48 hours with UV light from an ACE 7825-34 mercury vapor UV lamp (450 W). During this period, both tubes were kept at 4°C and rotated slowly.

After polymerization, the tubes were opened and the bulk polymer that formed was ground in short repeated cycles using an electric mill. Between each grinding cycle, the products were dry sieved through a 38-μm screen. The particles which passed through the sieve were collected and added to acetonitrile. The mixture was sonicated. After 30 min of sitting undisturbed, the supernatant liquid in which the finest particles were suspended was decanted and discarded while the sediment was saved. The same process was repeated three times. The sedimented particles were dried *in vacuo* at room temperature and then loaded into a cellulose Soxhlet thimble. The template and a small amount of other soluble residue were extracted from the resin over 24 hours using 100 mL acetonitrile-acetic acid (4:1, v/v). A second Soxhlet extraction with 100 mL acetonitrile was performed over another 24 hours to remove the acid. The washing solutions were saved for analysis by a Perkin-Elmer Lambda 35 UV/Vis spectrophotometer, and the polymers were obtained for further study after drying *in vacuo* at room temperature. These imprinted resins are designated MIP4HBA. Micrographs of the MIP4HBA particles were obtained using an Amray Model 1810 scanning electron microscope.

Batch Analysis of MIP4HBA and NIP

Portions of the MIP4HBA were added one at a time to acetonitrile solutions of 4HBA, 3HBA, or BA. The phase ratio was a commonly used one: 0.01 g solid/1 mL solution (3,26,31,32). The process was repeated with NIP for comparison. In separate experiments, pure solvent was added to MIP4HBA or NIP to determine if any template remained after the extraction. Each resin mixture was stirred for 24 hours at room temperature. After centrifugation, the supernatant was transferred into a scintillation vial through a 0.45-μm syringe filter. Because 4HBA, 3HBA, and BA acetonitrile solutions have their maximum UV absorbance

at 251 nm, 294 nm, and 225 nm, respectively, the concentration of free 4HBA in the supernatant was determined by measuring its UV absorbance at 251 nm; 3HBA, at 294 nm; and BA, at 225 nm.

RESULTS AND DISCUSSION

Hydrogen Bonding Between 4HBA and AA

The selectivity and affinity of MIPs are mainly affected by the interactions between the monomer and the template. Therefore, an understanding of the physical and chemical processes governing the formation of monomer-template complexes in the imprinting process and the subsequent recognition is fundamental for the design of MIPs. Lübke and coworkers proposed (33) that the structure of the template-functional monomer complex existing in solution prior to polymerization remains unchanged during polymerization and the resulting sites are not modified by shrinkage upon the template removal.

A ^{1}H-NMR titration experiment gave evidence for the hydrogen bonding (34) between the template and the monomer before the polymerization. From the NMR spectra of AA in deuterated acetonitrile, broadening of the two amide protons peaks in AA by proton exchange is evident. The chemical shifts of AA's two amide protons increased with the increasing concentrations of AA. We attribute these shifts to the increasing amount of hydrogen bonding as the AA solutions become more concentrated. 4HBA was added to these solutions to make all of them 0.05 mol/L in 4HBA. The chemical shifts increased with the addition of 4HBA as would be expected if 4HBA hydrogen bonded to the amide protons of AA. Figure 1 shows a comparison of the two sets of NMR spectra. Consistent with the conclusion that the 4HBA forms hydrogen bonds with AA, the effect of adding 4HBA to AA solutions is greatest in dilute solutions where the fraction of hydrogen bonds with 4HBA would be the greatest. Possible hydrogen bonds between 4HBA and AA were shown by Serena Software, PC Model (Version 5.13) in Fig. 2, in which the molecular models of 4HBA and AA in a minimum energy conformation were simulated using the MP3 method and their assembled space structure was optimized until the energy of the system was minimized.

Preparation of MIP4HBA

The MIP resins were prepared using a free-radical polymerization initiated with UV light. A white solid first appeared after the reactants had been irradiated for three hours. In the case of MIP4HBA, 90% of the template that was initially present in the reaction mixture was extracted from the washings of the resulting resin, as determined by UV/Vis spectrometry.

Scanning electron micrographs reveal the size and texture of MIP4HBA particles. The particle sizes were controlled by sieving and sedimentation. Their shapes were irregular (Fig. 3(a)). MIP4HBA showed a rough surface, the darker areas being pores (Fig. 3(b)).

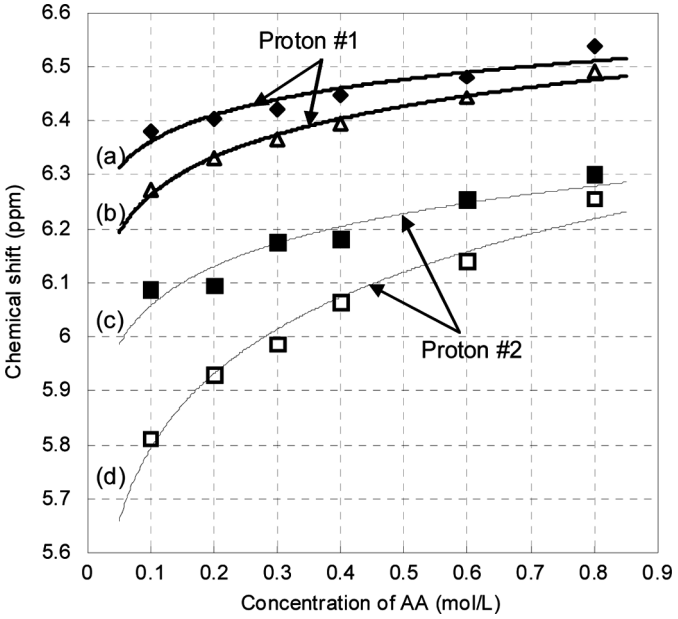

FIG. 1. Chemical shifts for the two amide protons in AA as a function of the concentration of AA. The upper curve (a) for "Proton #1" obtained for 0.05 mol/L 4HBA is compared with the lower curve (b) obtained for AA in the absence of 4HBA. Curves (c) and (d) are the corresponding shifts for "Proton #2". The lines were drawn arbitrarily through the data points.

Substrate Selectivity of MIP4HBA and NIP

The selectivity of MIP4HBA for different substrates was studied by measuring the resin's capacity for absorbing 3HBA and BA, both of which are related structurally to the 4HBA template (see Fig. 4). In carrying out this particular study, batch analyses were performed with both MIP4HBA and NIP resins.

The effects of molecular structure on binding affinities in MIP are apparent in a comparison of the binding of the three species in Fig. 5 to NIP and to MIP. 4HBA, 3HBA, and BA bind almost equally to NIP as shown in Fig. 5(a). Their saturation concentration on the NIP

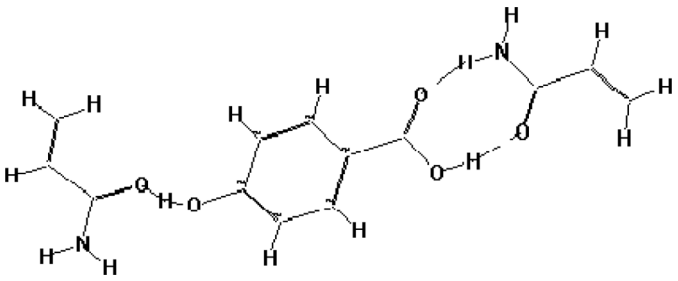

FIG. 2. Probable hydrogen bonding between 4HBA and AA.

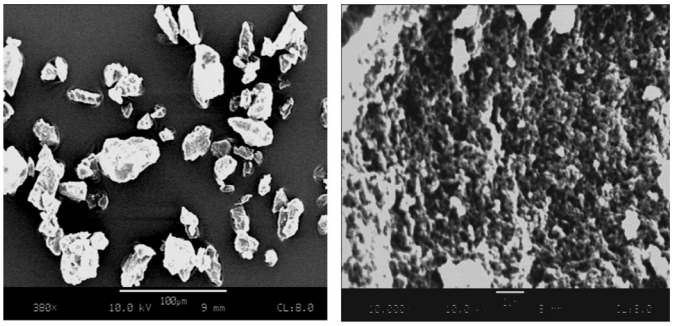

(a) (b)

FIG. 3. Scanning electron micrographs of MIP4HBA particles at (a) 380× and (b) 10,000× magnification.

appears to be just above 4 μmol/g. However, in experiments with MIP as shown in Fig. 5(b), 4HBA (the template) was bound to a greater extent than either 3HBA or BA, with greater binding by BA compared to 3HBA. The MIP was not saturated by any of the three analytes over the ranges of solution concentrations used.

After the first rebinding of 4HBA, 4HBA was extracted again from MIP4HBA and NIP resins. Then the dried resins were stored at room temperature for two months. A second set of rebinding experiments was carried out with the same resins and under the same experimental conditions for comparison. Very similar results were obtained, showing MIP's stability and robustness.

Comparison of Batch Analysis and Chromatographic Evaluation

Zhang et al. (32) used a 4HBA imprinted resin for the stationary phase in a liquid chromatographic separation of 4HBA, 3HBA, and BA. Their column not only separated 4HBA from the structurally similar compounds, but also had a higher capacity and greater relative retention for 4HBA than for 3HBA and BA (Table 1). Values for selectivity and imprinting efficacy from the current equilibrium binding experiments are compared in Table 1. We find evidence for greater selectivity in our equilibrium binding measurements than Zhang et al. (32) This is because, in the chromatographic analysis, the absorption-adsorption between the analyte and the binding sites does not reach

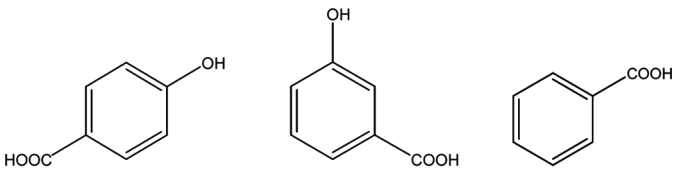

(a) (b) (c)

FIG. 4. Structures of the substrates used: (a) 4HBA, (b) 3HBA, and (c) BA.

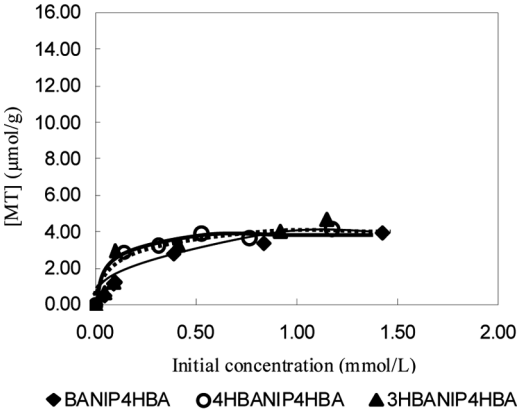

(a)

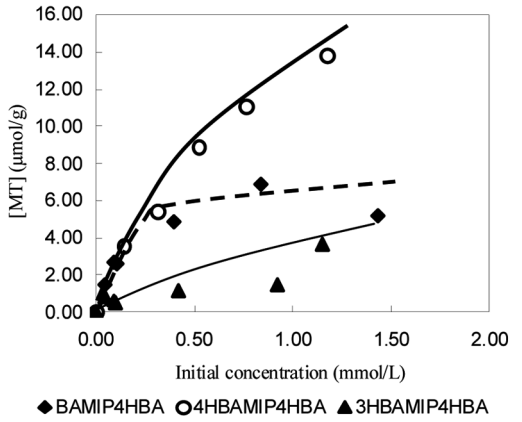

(b)

FIG. 5. Binding isotherms of 4HBA, 3HBA, and BA on (a) NIP and (b) MIP4HBA. [MT], the concentration of BA or 4HBA or 3HBA bound to 0.1 g NIP or MIP4HBA (μmol/g of resin) at equilibrium. Concentration of resin in solution: 0.01 g/1.0 mL; binding time: 24 hours; temperature: 25°C.

equilibrium; whereas, in the batch experiment, the binding is an equilibrium process. However, both experiments showed that MIP has a significant imprinting performance.

Binding Analyses of MIP4HBA and NIP Resins

The substrate's binding process can be described as an equilibrium:

$$M + T \rightleftharpoons MT$$

where [M] is defined as the concentration of empty sites in the resin at equilibrium (mmol of empty sites/g of resin); [T], the concentration of substrate in solution at equilibrium (mmol/L); and [MT], the concentration of substrate bound in the resin at equilibrium (μmol/g of resin), with the latter calculated from the difference between the moles of the free substrate and the initial quantity of the substrate.

TABLE 1
The selectivity factors from MIP4HBA binding experiment and its chromatographic evaluation (32).[a]

Binding evaluation (this work)	4HBA	3HBA	BA	Chromatographic evaluation (32)	4HBA	3HBA	BA
$\alpha_{MIP4HBA}{}^{b}$	1	10.71	2.42	$\alpha'_{MIP4HBA}{}^{b}$	1	2.23	7.26
$\alpha_{NIP}{}^{b}$	1	1.08	3	$\alpha'_{NIP}{}^{b}$	1	0.94	2.29
β^{b}	1	9.92	0.81	β'^{b}	5.51	2.32	1.74

[a]Experimental conditions: for comparison, the concentration for the binding solution of 0.1 mmol/mL was selected as the same as the injected solution's concentration used for HPLC. 0.1 g MIP or NIP was incubated in 10 mL of 0.1 mmol/L binding solution.

[b]In the binding evaluation, the selectivity factor α is defined as $\alpha =$ (amount of 4HBA absorbed)/(amount of analyte absorbed) and the molecular imprinting efficacy factor β is defined as $\beta = \alpha_{MIP}/\alpha_{NIP}$; in the chromatographic evaluation, the capacity factor $k' = (t_R - t_0)/t_0$, where t_R and t_0 are the retention time of the sample and the void marker, respectively; the relative retention value $\alpha' = k'_t/k'_i$, the ratio of capacity factors for any two substances on the same column; and the molecular imprinting factor $\beta' = k'_{MIP}/k'_{NIP}$.

The relationship among these quantities can be expressed as the Scatchard equation (35):

$$\frac{[MT]}{[T]} = -K_a[MT] + K_a[MT]_{max} \quad (1)$$

with the assumption that all the substrate-binding sites in an MIP are identical. $K_a = [MT]/([M][T])$ and $[MT]_{max}$ represent the association constant for MT and the maximum number of binding sites per unit mass of the resin, respectively.

In accordance with common practice, the porogen acetonitrile used in the polymerization was used as the solvent for the batch analyses (36,37). After the imprinted (MIP) and non-imprinted (NIP) resins had been subjected to the extraction, they were immersed in 4HBA-acetonitrile solutions whose concentrations were varied over the range 0–2.0 mmol/L. The binding isotherms for 4HBA in both resins, as determined from the UV-absorbance of the solutions, are compared in Fig. 6. The MIP absorbed more 4HBA than did an equal mass of NIP with the difference increasing with increasing concentration.

The experimental data in Fig. 6 are re-plotted in Fig. 7 with [MT]/[T] graphed as a function of [MT]. For the NIP, the ratio [MT]/[T] is taken to be a linear function of [MT] over the range from $[MT] = 0$ to a concentration approaching saturation of the resin. The slope and intercept of the line representing these data were determined by the method of least squares, with each point weighted in proportion to the inverse square of its experimental uncertainty (38). The large uncertainties in [MT]/[T] are a consequence of taking the differences between pairs of small concentrations. The results for NIP yield the equilibrium association constant $K_{a,NIP} = (4.4 \pm 0.2)$ (mmol/L)$^{-1}$ and the maximum number of binding sites $[MT]_{max,NIP} = (6.7 \pm 0.3)$ μmol/g.

The data in Fig. 7 for MIP4HBA solutions are not linear, but concave upwards. To take account of the nonlinearity of the MIP4HBA data in Fig. 7, the imprinted resin was treated as having two kinds of binding sites with different affinities: "general" sites which in this system dominate the behavior at low concentrations of template species, and "special" binding sites, dominant at high concentrations. The general binding sites were assumed to be the same as those found in the NIP resin. Accordingly, they are assigned the same affinity constant $K_{a,g} = K_{a,NIP}$ and the same site density $[MT]_{max,g} = [MT]_{max,NIP}$, both of which are listed under "general" in Table 2.

According to this model, some of the bound template is adsorbed on the general sites in the MIP4HBA resin while the remainder of the bound template is found on the special sites. The concentration of occupied general binding sites

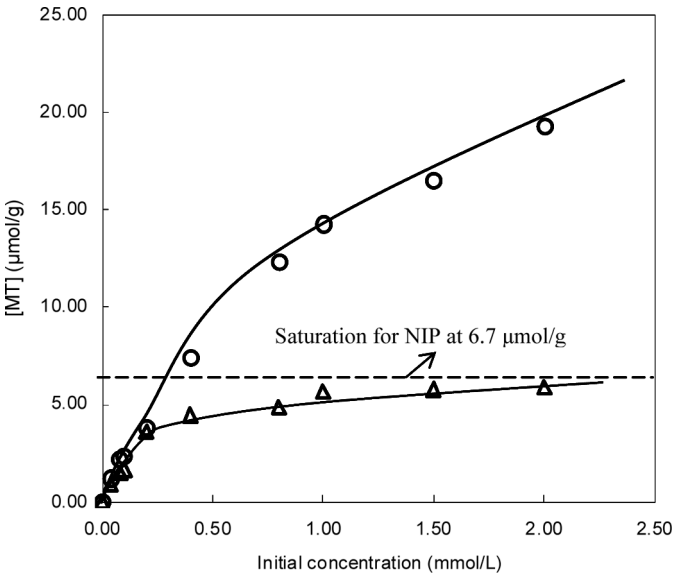

FIG. 6. Binding isotherms for 4HBA on MIP4HBA and NIP at 25°C with an incubation time of 24 hours. [MT], the concentration of 4HBA bound to 0.1 g NIP or MIP4HBA at equilibrium (μmol/g of resin). The dashed line at $[MT] = [MT]_{max,NIP} = 6.7$ μmol/g is the asymptotic limit for NIP as explained in the text.

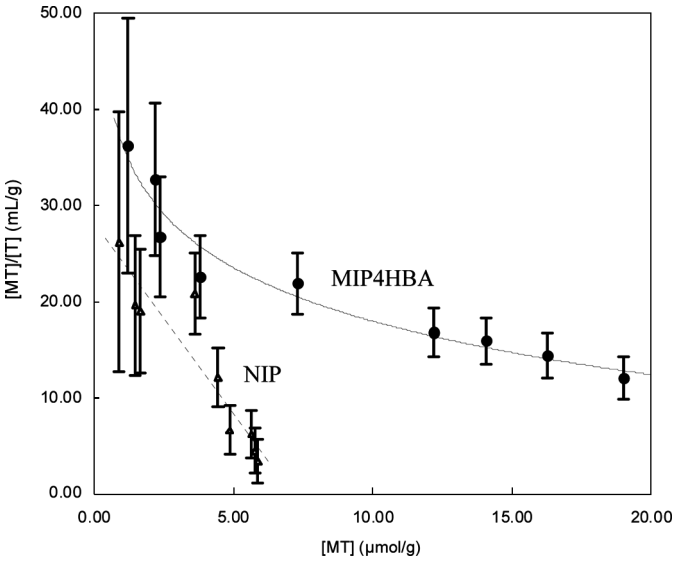

FIG. 7. Scatchard plots of MIP4HBA (filled circles) and NIP (open triangles) for 4HBA. Both lines are trend lines for the experimental data.

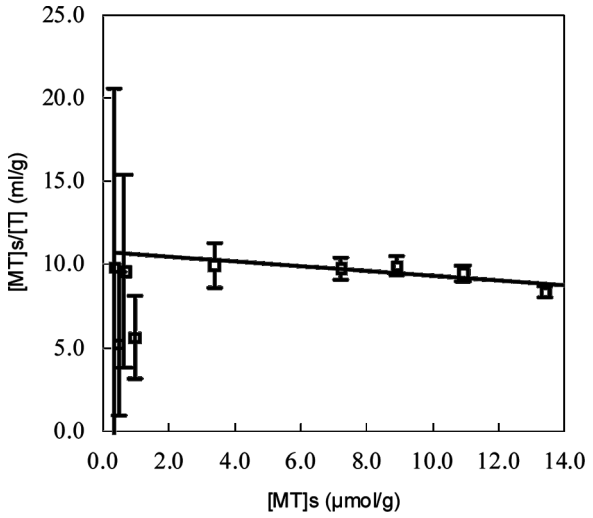

FIG. 8. Scatchard plot for the special binding sites with $[MT]_s$ determined using Eq. (4).

$[MT]_g$ for a given [T] can be calculated from $K_{a,g}$ and $[MT]_{max,g}$ using the results of measurements on NIP and Eq. (2).

$$[MT]_g = \frac{K_{a,g}[MT]_{max,g}[T]}{1 + K_{a,g}[T]} \tag{2}$$

The concentration of occupied special sites $[MT]_s$ in the imprinted resin is the difference between $[MT]_{total}$, obtained from measurements on MIP and $[MT]_g$.

$$[MT]_s = [MT]_{total} - [MT]_g = [MT]_{total} - \frac{K_{a,g}[MT]_{max,g}[T]}{1 + K_{a,g}[T]} \tag{3}$$

According to the Scatchard plot of the special-site data determined from Eq. (3) (Fig. 8), the behavior of the special binding sites is also assumed to follow the Scatchard model so that

$$\frac{[MT]_s}{[T]} = -K_{a,s}[MT]_s + K_{a,s}[MT]_{max,s}. \tag{4}$$

TABLE 2
Comparison of the general and special sites in MIP4HBA resin

Sites type	K_a $(mmol/L)^{-1}$	$[MT]_{max}$ (μ mol/g)
General	4.4 ± 0.2	6.7 ± 0.3
Special	0.15 ± 0.01	75 ± 2

Substitution in Eq. (3) for $K_{a,g}$ and $[MT]_{max,g}$ from the non-imprinted results yielded values for the concentration of the occupied special sites $[MT]_s$ in the imprinted resin. The latter are plotted in Fig. 8 in the form suggested by Eq. (4).

From the slope and intercept of the linear least-square line in Fig. 8, $K_{a,s}$ and $[MT]_{max,s}$ were evaluated (Table 2). These values and those determined from the NIP resin were

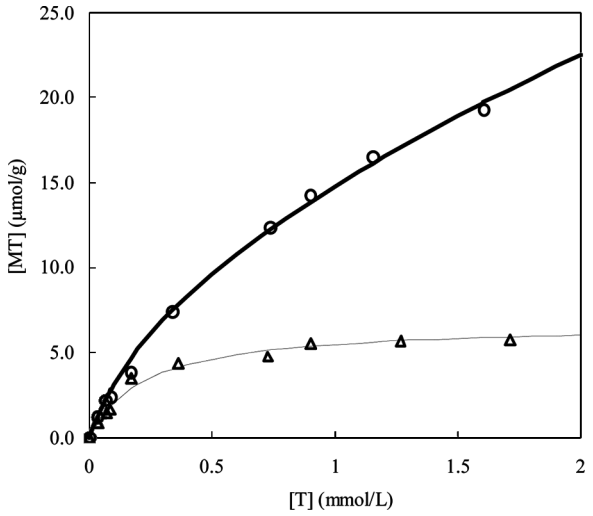

FIG. 9. [MT] vs. [T]. [T], concentration of 4HBA in solution at equilibrium (mmol/L). [MT], concentration of 4HBA bound to 0.1 g NIP or MIP4HBA at equilibrium (μmol/g of resin). The circles and the triangles are calculated based on the experimental data for MIP4HBA and NIP resins, respectively. The solid line in bold is a plot of the uptake of MIP4HBA as calculated from Eq. (5); another solid line is a plot of the uptake by the NIP resin as calculated from Eq. (2).

substituted in Eq. (5):

$$[\mathrm{MT}]_{\mathrm{total}} = [\mathrm{MT}]_{\mathrm{s}} + [\mathrm{MT}]_{\mathrm{g}} = \frac{K_{a,\mathrm{s}}[\mathrm{MT}]_{\mathrm{max,s}}[\mathrm{T}]}{1 + K_{a,\mathrm{s}}[\mathrm{T}]} + \frac{K_{a,\mathrm{g}}[\mathrm{MT}]_{\mathrm{max,g}}[\mathrm{T}]}{1 + K_{a,\mathrm{g}}[\mathrm{T}]}. \quad (5)$$

The ability of this two-site model to predict the binding behavior in this system was demonstrated in Fig. 9. The two solid lines in the same figure were drawn using Eqs. (2) and (5). The upper solid line in bold is for 4HBA in the presence of a resin imprinted with 4HBA. The lower line was drawn for 4HBA in the non-imprinted resin, i.e., a resin with no special sites and $[\mathrm{MT}]_{\mathrm{max,s}} = 0$. The differences between the data points and the lines lie within the uncertainties of the observed values.

Comparison of the General and Special Binding Sites in MIP4HBA

With this two-site model, $K_{a,\mathrm{g}} > K_{a,\mathrm{s}}$, the same phenomenon was reported in our previous study of 3HBA imprinted resins (39). Thus, the decrease in the Gibbs energy for binding at general sites exceeds that for binding at special sites. If the binding energy between the analyte and the resin is greater at the special sites than at the general sites, then it follows that the entropy loss is greater at the special sites. This is consistent with the general understanding that binding at special sites is constrained by the sizes, shapes, and orientations of the binding sites and the analyte molecules.

The density of special sites $[\mathrm{MT}]_{\mathrm{max,s}} = 75\,\mu\mathrm{mol/g}$ was found to be about half the number of template molecules ($160\,\mu\mathrm{mol/g}$) per gram of monomer and crosslinker used in the polymerization. The earlier study with MIP3HBA (39) yielded similar results $K_{a,\mathrm{g}} > K_{a,\mathrm{s}}$ and $[\mathrm{MT}]_{\mathrm{max,g}} < [\mathrm{MT}]_{\mathrm{max,s}}$.

CONCLUSIONS

Binding analyses of 4HBA-imprinted resins showed a special affinity for the *para*-substituted 4-hydroxybenzoic acid, but not for its *meta*-substituted isomer, nor for benzoic acid. These results show that an imprinted resin's recognition ability is dependent on the target's size, shape, and functionality.

The studies described here incorporate the effects of binding that are found in NIP as well as in MIP resins. A two-binding-site Scatchard model is proposed for the imprinted resin: *general* sites, the same as those found in the non-imprinted resin, and *special* sites in the imprinted resin, the result of imprinting by the template species. The parameters $[\mathrm{MT}]_{\mathrm{max,NIP}}$ and $K_{a,\ \mathrm{NIP}}$ taken directly from measurements on the non-imprinted resin characterize the general sites in the imprinted resin. The special sites in the MIP are assigned values for $[\mathrm{MT}]_{\mathrm{max,s}}$ and $K_{a,\mathrm{s}}$ after the effects of the general sites in the imprinted resin have been subtracted from the total binding. These results were not obtained by simply subtracting one Scatchard plot from another. Rather, the new binding isotherm for the special binding sites was subtracted from that of the MIP system. While the binding energy for the template species in imprinted resins is presumed to be greater at the special sites than at the general sites, the orientational limitations in the analyte molecule's binding result in an equilibrium constant for binding at the special sites being less than that for binding at the general sites.

Binding by the two isomers 4HBA and 3HBA and by benzoic acid is similar in the NIP and at the general sites in the MIP.

REFERENCES

1. Yu, Y.; Ye, L.; Haupt, K.; Mosbach, K. (2002) Formation of a class of enzyme inhibitors (drugs), including a chiral compound, by using imprinted polymers or biomolecules as molecular-scale reaction vessels. *Angew Chem. Int. Ed.*, 41: 4459.
2. Sellergren, B. (2010) Molecularly imprinted polymers: shaping enzyme inhibitors. *Nature Chemistry*, 2 (1): 7.
3. Zhu, Q.Z.; Haupt, K.; Knopp, D.; Niessner, R. (2002) Molecularly imprinted polymer for metsulfuron-methyl and its binding characteristics for sulfonylurea herbicides. *Anal. Chim. Acta*, 468 (2): 217.
4. Kueseng, P.; Noir, M.L.; Mattiasson, B.; Thavarungkul, P.; Kanatharana, P. (2009) Molecularly imprinted polymer for analysis of trace atrazine herbicide in water. *Journal of Environmental Science and Health, Part B: Pesticides, Food Contaminants, and Agricultural Wastes*, 44 (8): 772.
5. Murray, G.M. (2003) Polymer based Permeable Membrane for Removal of Ions. U.S. Patent 2003-0113234 (A1), June 19, 2003.
6. Aherne, A.; Alexander, C.; Payne, M.J.; Perez, N.; Vulfson, E.N. (1996) Bacteria-mediated lithography of polymer surfaces. *J. Am. Chem. Soc.*, 118 (36): 8771.
7. Fu, Q.; Sanbe, H.; Kagawa, C.; Kunimoto, K.; Haginaka, J. (2003) Uniformly sized molecularly imprinted polymer for (*s*)-nilvadipine comparison of chiral recognition ability with HPLC chiral stationary phases based on a protein. *Anal. Chem.*, 75 (2): 191.
8. Takeuchi, T.; Hishiya, T. (2008) Molecular imprinting of proteins emerging as a tool for protein recognition. *Organic & Biomolecular Chemistry*, 6 (14): 2459.
9. Hishiya, T.; Asanuma, H.; Komiyama, M. (2002) Spectroscopic anatomy of molecular-imprinting of cyclodextrin. Evidence for preferential formation of ordered cyclodextrin assemblies. *J. Am. Chem. Soc.*, 124 (4): 570.
10. Titirici, M.M.; Hall, A.J.; Sellergren, B. (2003) Hierarchical imprinting using crude solid phase peptide synthesis products as templates. *Chemistry of Materials*, 15 (4): 822.
11. Wei, S.; Jakusch, M.; Mizaikoff, B. (2006) Capturing molecules with templated materials – Analysis and rational design of molecularly imprinted polymers. *Anal. Chim. Acta*, 578 (1): 50.
12. Shinkai, S.; Takeuchi, M. (2004) Molecular design of synthetic receptors with dynamic, imprinting, and allosteric functions. *Biosensors & Bioelectronics*, 20 (6): 1250.
13. Turkewitsch, P.; Wandelt, B.; Darling, G.D.; Powell, W.S. (1998) Fluorescent functional recognition sites through molecular imprinting. A polymer-based fluorescent chemosensor for aqueous cAMP. *Anal. Chem.*, 70 (13): 2771.

14. Dickert, F.L.; Tortschanoff, M.; Fischerauer, G.; Bulst, W.E. (1999) Molecularly imprinted sensor layers for the detection of polycyclic aromatic hydrocarbons in water. *Anal. Chem.*, 71 (20): 4559.
15. Haupt, K. (2003) Molecularly imprinted polymers: The next generation. *Anal. Chem.*, 75 (17): 376A.
16. Hu, L.Y. (2004) Binding studies of molecularly imprinted polymers. PhD Dissertation, College of William and Mary in Virginia.
17. Umpleby, R.J., II; Baxter, S.C.; Chen, Y.; Shah, R.N.; Shimizu, K.D. (2001) Characterization of molecularly imprinted polymers with the Langmuir-Freundlich isotherm. *Anal. Chem.*, 73 (19): 4584.
18. Umpleby, R.J., II; Bode, M.; Shimizu, K.D. (2002) Measurement of the continuous distribution of binding sites in molecularly imprinted polymers. *Analyst*, 125 (7): 1261.
19. Rampey, A.M., Umpleby, R.J., II; Rushton, G.T., Iseman, J.C., Shah, R.N., Shimizu, K.D. (2004) Characterization of the imprint effect and the influence of imprinting conditions on affinity, capacity, and heterogeneity in molecularly imprinted polymers using the Freundlich isotherm-affinity distribution analysis. *Anal. Chem.*, 76 (4): 1123.
20. Michailof, C.; Manesiotis, P.; Panayiotou, C. (2008) Synthesis of caffeic acid and *p*-hydroxybenzoic acid molecularly imprinted polymers and their application for the selective extraction of polyphenols from olive mill waste waters. *J. Chromatography, A*, 1182 (1): 25.
21. Yanez, F.; Chianella, I.; Piletsky, S.A.; Concheiro, A.; Alvarez-Lorenzo, C. (2010) Computational modeling and molecular imprinting for the development of acrylic polymers with high affinity for bile salts. *Anal. Chim. Acta*, 659: 178.
22. Mosbach, K.; Te, L.; Yu, Y. (2002) Process for clavulanic acid purification using molecular imprinted polymers. WO0222846 (A1), March 21, 2002.
23. Zhang, Z.; Liao, H.; Li, H.; Nie, L.; Yao, S. (2005) Stereoselective histidine sensor based on molecularly imprinted sol-gel films. *Analytical Biochemistry*, 336 (1): 108.
24. Lin, L.; Li, Y.; Fu, Q.; He, L.; Zhang, J.; Zhang, Q. (2006) Preparation of molecularly imprinted polymer for sinomenine and study on its molecular recognition mechanism. *Polymer*, 47 (11): 3792.
25. Xu, Z.; Kuang, D.; Liu, L.; Deng, Q. (2007) Selective adsorption of norfloxacin in aqueous media by an imprinted polymer based on hydrophobic and electrostatic interactions. *J. Pharmaceutical and Biomedical Analysis*, 45 (1): 54.
26. Hua, Z.; Chen, Z.; Li, Y.; Zhao, M. (2008) Thermosensitive and salt-sensitive molecularly imprinted hydrogel for bovine serum albumin. *Langmuir*, 24 (11): 5773.
27. Quaglia, M.; Chenon, K.; Hall, A.J.; De Lorenzi, E.; Sellergren, B. (2001) Target analogue imprinted polymers with affinity for folic acid and related compounds. *J. Am. Chem. Soc.*, 123 (10): 2146.
28. Shea, K.J.; Spivak, D.; Sellergren, B. (1993) Polymer complements to nucleotide bases – selective binding of adenine-derivatives to imprinted polymers. *J. Am. Chem. Soc.*, 115 (8): 3368.
29. Huang, X.; Kong, L.; Li, X.; Zheng, C.; Zou, H. (2003) Molecular imprinting of nitrophenol and hydroxybenzoic acid isomers: effect of molecular structure and acidity on imprinting. *J. Molecular Recognition*, 16 (6): 406.
30. Dmitrienko, S.G.; Irkha, V.V.; Duisebaeva, T.B.; Mikhailik, Y.V.; Zolotov, Y.A. (2006) Synthesis and study of the sorption properties of 4-hydroxybenzoic acid-imprinted polymers. *J. Anal. Chem.*, 61 (1): 14.
31. Katz, A.; Davis, M.E. (1999) Investigations into the mechanisms of molecular recognition with imprinted polymers. *Macromolecules*, 32 (12): 4113.
32. Zhang, T.; Liu, F.; Chen, W.; Wang, J.; Li, K. (2001) Influence of intramolecular hydrogen bond of templates on molecular recognition of molecularly imprinted polymers. *Anal. Chim. Acta*, 450 (1–2): 53.
33. Lübke, C.; Lübke, M.; Whitecombe, M.J.; Vulfson, E.N. (2000) Imprinted polymers prepared with stoichimetric template-monomer complexes: Efficient binding of ampicillin from aqueous solutions. *Macromolecules*, 33 (14): 5098.
34. Rebek, J.; Askew, B.; Killoran, M.; Nemeth, D.; Lin, F.T. (1987) Convergent functional groups. 3. A molecular cleft recognizes substrates of complementary size, shape, and functionality. *J. Am. Chem. Soc.*, 109 (8): 2426.
35. Yamamura, H.I.; Kuhar, M.J. (1985) *Neurotranmitter, Receptor Binding*, 2nd ed.; Raven Press: New York.
36. Spivak, D.; Gilmore, M.A.; Shea, K. (1997) Evaluation of binding and origins of specificity of 9-ethyladenine imprinted polymers. *J. Am. Chem. Soc.*, 119 (19): 4388.
37. Armstrong, D.W.; Schneiderheinze, J.M.; Hwang, Y.S.; Sellergren, B. (1998) Bubble fractionation of enatiomers from solution using molecularly imprinted polymers as collectors. *Anal. Chem.*, 70 (17): 3717.
38. Garland, C.W.; Niber, J.W.; Shoemaker, D.P. (2003) *Experiments in Physical Chemistry*, 7th ed.; The McGraw-Hill Companies, Inc.
39. Hu, Y.; Orwoll, R.A. (2004) Molecular imprinting of 3-hydroxybenzoic acid: special and general binding sites. *Materials Research Society Symposium Proceedings*, 787 (Molecularly Imprinted Materials–2003), 41.